Parallel 3D simulation of seismic wave propagation: Observation and simulation

Takashi Furumura

Earthquake Research Institute, University of Tokyo, 1-1-1 Yayoi, Bunkyoku 113-0032, Japan, (e-mail: furumura@eri.u-tokyo.ac.jp, phone: +81 3 5841 5777, fax: +81 3 5689 7265)

Abstract

A dense seismic network of strong ground motion instruments in Japan allows detail characterization of regional wave propagation during large earthquakes. Steadily improving computer power associated with sophisticated parallel algorithms realizes large scale computer simulation of seismic waves in 3D structure. The link between the array observation and high-resolution computer simulation provide a key to the understanding of the complex wave behavior imposed by the heterogeneous source and crustal structure along the propagation path. For the 2000 Tottori-ken Seibu earthquake (Mw 6.6) in western Japan, snapshots of ground motion, derived from the dense array observations, and numerical modeling of seismic wave propagation demonstrate clearly the source radiation and the character of the regional seismic wavefield during the earthquake.

Introduction

Over the last few years very dense arrays of strong ground motion instruments K-NET (Kinoshita, 1998) and KiK-net (Aoi et al., 2000) have been deployed across Japan by NIED, and we now have over 1600 strong motion instruments at a nearly uniform station interval of 10 to 20 km.

The development of such a dense array means that is is feasible to visualize the behavior of seismic wave propagation across heterogeneous crust and upper-mantle structure of the Japanese Island. Huang (2000) used 650 nation-wide strong motion network in Taiwan to illustrate the seismic radiation and propagation characteristics during the 1999 Chi-Chi, Taiwan (Mw 7.5) earthquake. Koketsu and Kikuchi (2000) combined data from 400 strong motion accelerograph and seismic intensity meters in the Kanto, Japan area to study the complicated wave propagation character of the Love waves in the Kanto basin. Following these studies we will make use of the array data from the 2000 Tottori-ken Seibu (Mw 6.6) earthquake to understand the regional seismic wavefield in western Japan during the earthquake. To compliment the observation we then conduct numerical 3D simulation of seismic wave propagation using a newly developed multigrid parallel hybrid PSM/FDM code.

The 2000 Tottori-ken Seibu earthquake (Mw6.6)

The Tottori-ken Seibu earthquake (Mw6.6) of 16 Oct. 2000 was the largest damaging event since the destructive 1995 Hyogo-ken Nanbu (Kobe) earthquake (Mw 6.9) which also occurred at western Japan. The ground shaking during the 2000 event was well recorded at 520 K-NET and KiK-net stations.

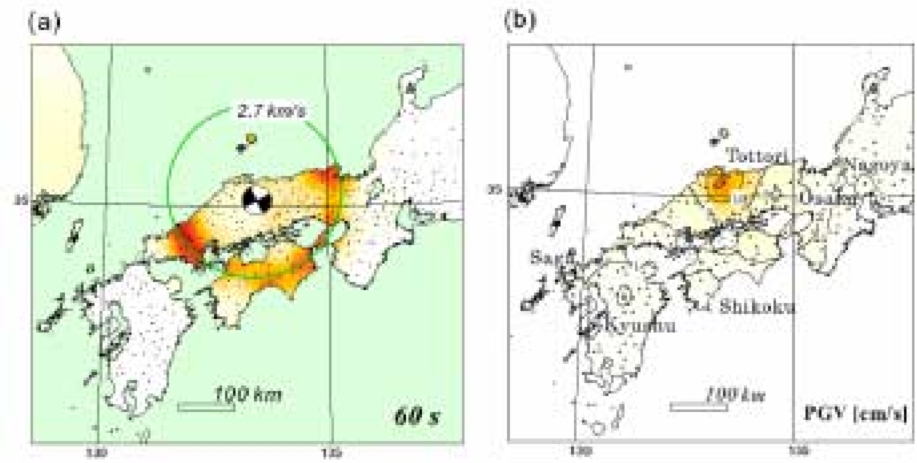

Figure 1: (a) Snapshot of seismic wave propagation during the 2000 Tottori-ken Seibu earthquake at 60 s from the source initiation, derived from the digital records of strong ground motion stations. The green circle indicates propagation speed of V=2.7 km/s. (b) Peak ground velocity (cm/s) during the earthquake. The KiK-net strong motions stations are shown by triangles.

Figure 1a illustrates a snapshot of seismic wave propagation at 60 s from the fault rupture initiation, produced from the interpolation of observed records after applying an antialias filter with a cut-off frequency of 0.25 Hz. A large seismic energy propagating at a speed of around 2.7 km/s, which corresponds to the group velocity of the fundamental-mode Love wave, is clearly seen in the snapshot. The shallow (H=11 km) strike-slip fault source radiates large amplitude *SH* wave to NE--EW and its orthogonal directions, so the Love wave dominates in these directions. Observed waveforms also indicate that the short-period *Lg* wave, as a sum of post-critical *SmS* reflections in the crustal waveguide, was also a prominent feature in the short-period regional wavefield (see, Furumura and Kennett, 2001, Kennett and Furumura, 2002).

The distribution of peak ground velocity (PGV) during the earthquake is shown in Fig. 1b, indicating that longer-period velocity wavefield is characterized, in most parts, by the propagation of the Love wave and local ground conditions. The Love wave propagating into the basin structure is amplified significantly by the low-velocity materials overlaying the high-velocity bedrock, and the waveshape is elongated considerably by dispersion and scattering in the heterogeneous structure Larger and longer ground shaking is found at highly populated cities such as at e.g. Osaka, Nagoya and Saga.

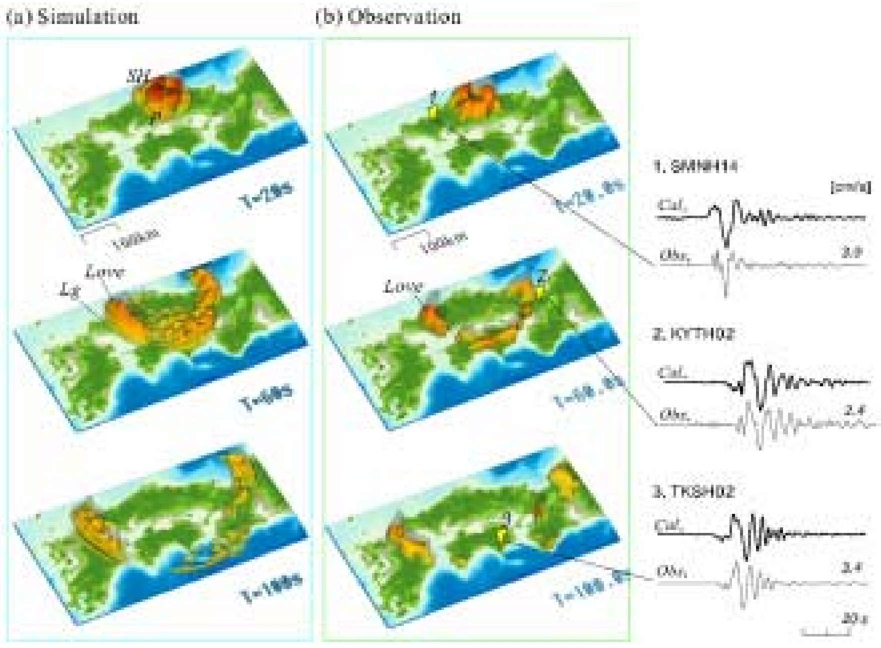

Figure 2: Snapshots of seismic wave propagation for horizontal ground motion during the 2000 Tottori-ken Seibu earthquake comparing between (a) simulation result and (b) observed wavefield. The seismograms from simulation (Cal.) and observation (Obs.) at three stations are also comparing in the right.

Numerical 3D Simulation of the 2000 Tottori-ken Seibu earthquake

To compliment the observation we then conduct numerical modeling of seismic wave propagation for the 2000 Tottori-ken Seibu earthquake using the hybrid PSM/FDM code (Furumura et al., 2000, 2002). This modeling scheme uses the accurate Fourier spectral method (PSM) in horizontal (x-y) planes, and a conventional fourth-order staggered-grid finite-difference method (FDM) in vertical (z) direction. The advantage of such a hybrid approach is that the inter-processor communications consumed for parallel computing is minimized compared with the parallel PSM.

The 3D structural model for the western Japan is constructed by a number of data sets from e.g., *P*-wave travel-time tomography data (Zhao and Hasegawa, 1993), *S*-wave velocities derived from the dispersion analysis of the Love waves, the distribution of Moho depth (Ryoki, 1999) and the depth of the top of the Philippine Sea-plate (Ishida, 1989). We assigned a relatively low *S*-wave velocity (Vs=2.1 km/s) and a low *Q* (*Q*=80) to the upper 2 km material of the basins.

The source model employed here is derived from an inversion of strong motion data and teleseismic waveforms (Yagi and Kikuchi, 2000), which is represented by one large fault plane cutting from south to north associated by two small branches to the west and north. On the main segment a larger slip of over 2.5m occurred just above the hypocenter at 2km depth. The fault rupture is represented by a set of point sources arranged on the fault plane, which impart seismic wave with a maximum frequency of 1Hz.

The simulation model covers the zone of 819 km by 409 km by 167 km, which is discritized with a horizontal mesh increment of 1.6 km and a vertical increment of 0.8 km. The embedded finer mesh model is 4 km thick with a smaller mesh increment of 0.8 km by 0.8 km by 0.4 km. Using this multigrid model, small-scale near-surface heterogeneities are efficiently incorporated in the large scale 3D model. To allow the wave propagation through two domains, an accurate interpolation procedure based on the Fourier transform is used to connect two wavefields with different grid intervals.

The parallel 3D simulation required 5 GB memory and a wall-clock time of 2 hours using 128 CPUs of the HITACHI SR8000/MPP or 20 hours using a PC Cluster of four 2.2 GHz Intel Xeon PCs (8CPUs in total) connected by a Gigabit Ethernet local network.

Figure 2 comparing the simulated ground velocity derived from the 3D simulation with the corresponding snapshots of the observed ground motions.

In the first snapshot at 20 s from the source initiation, four-robe pattern of the large amplitude *SH* waves from the shallow right-lateral strike-slip fault source is clearly seen. In the second frame at 40 s the Love waves built up from the *SH* waves, and the *Lg* wave begins to separate from the rest of the *S*-wave energy. The fundamental-mode Love wave is the prominent feature in the regional wavefield propagating at a group velocity of at 2.8 km/s following a *Lg* wave at a group velocity around 3.5 km/s. As the Love wave entering the basin structure the waveshape disrupts significantly by scattering and dispersions in the shallow heterogeneous structure. The long ground shaking in the basin structure illuminate the outline of the basin shape for longer time (see 100 s frame).

We display a comparison of simulated and observed waveforms of ground velocity for tangential component at three KiK-net stations (KYTH02, SMNH14, and TKSH02). The feature of the observed velocities are reproduced by the numerical simulation quite well, indicating the effectiveness of the 3D structure model for western Japan.

Strong Motion Simulation for the Nankai Trough Earthquakes

We therefore applied the model to simulating strong ground motions expected for Nankai Trough megathrust earthquakes, represented by a shallow angle thrust faulting over the subducting Philippine-sea plate. The long documented history back to 684 A.D. indicates that huge (M 8) earthquake occurs recurrently along the Nankai Trough at every 100 to 200 years.

Figure 3a shows a display of the ground velocity motions for the 1944 Tonankai (M 8) earthquake derived by the 3D simulation using a source model of Kikuchi et al. (1999). The unilateral fault rupture running from SW to NE radiate larger seismic energy to east, developing a large and long-period pulse to east. The estimated seismic intensity of the Japan Meteorological Agency (JMA) scale (maximum of seven) is shown in the Fig. 3, demonstrating larger ground motions of seismic intensities of four or larger at the eastern side of the fault. The pattern of the seismic intensity distribution derived by the simulation agrees to the observation for the 1944 Tonankai earthquake fairly well.

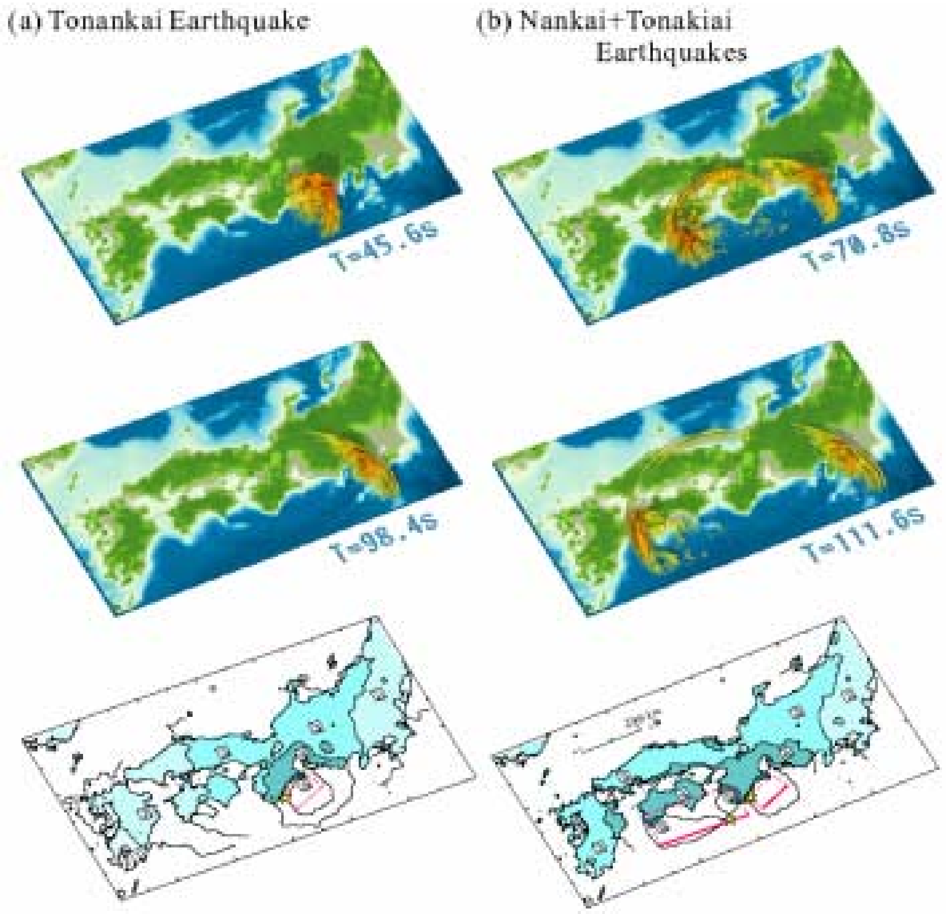

Figure 3: Snapshots of seismic wave propagation from (a) the 1944 Tonankai and (b) an expected megathrust earthquake from Nankai to Tonankai seismic zones. Expected seismic intensity of the JMA scale for these earthquake are shown at the bottom. Stars and squares indicate the hypocenter and the source areas for the Nankai and the Tonankai Earthquakes.

We also conducted a numerical modeling of strong ground motions for another scenario event which assumes that the fault rupture runs bilaterally to Tonankai and Nankai area simultaneously. This was the case during the 1707 Hoei event. We combine the source-slip model for the 1946 Nankai event (M 8) (Yamanaka et al., 2001) and the 1944 event, and the fault rupture is assumed to starts at the center of the two fault planes.

Figure 3b shows potential impact of this earthquake in terms of the ground motions at each time and the JMA seismic intensities during the earthquake. An elongated area of larger ground motions of JMA intensity of four or larger is found from Kyushu to Tokyo along the large fault plane.

Conclusion

It is well recognized that the seismic wavefield is controlled by the radiation from the earthquake and is then significantly affected by the variations in the crust and upper mantle structures along the propagation paths. Thus, to consider the strong ground motion behavior for future events we need a detailed understanding of the regional wavefield and its relation between the 3D structure.

We can expect that recent developments of dense strong motion network across Japan and computer simulation technology recover such information. As illustrated in the present article the dense array observation realizes the direct visualization of the wavefield generated during large earthquake. At the same time, recent powerful parallel computer allows realistic 3D modeling of regional wave propagation for frequencies close to 1 Hz.

Thus, the prediction of strong ground motion patterns expected for future earthquakes will depend on maintaining a close link between the seismological observations and the computer simulation.

Acknowledgments

This study is supported by Earth Simulator Project of Ministry of Education, Culture, Sports and Technology. The computation is conducted at Earthquake Information Center, Earthquake Research Institute, University of Tokyo and at Super Computer Center, University of Tokyo. K-net and KiK-net data are made available by the National Institute for Earth Science and Disaster Research (NIED), Japan.

References

[1] Aoi, S., S. Obara, S. Hori, K. Kasahara and Y. Okada, 2000, New strong-motion observation network: KiK-net, EOS Trans. Am. Geophys. Union, 81, F863.

[2] Furumura, T., and B.L.N. Kennett, 2001, *Variations in regional phase propagation in the area around Japan,* Bull. Seism. Soc. Am., **91**, 667--682.

[3] Furumura, T., K. Koketsu and H. Takenaka, 2000, *A hybrid PSM/FDM parallel simulation for 3-D seismic (acoustic) wavefield,* Butsuri-Tansa (J. SEGJ), **53**, 294--308, in Japanese

[4] Furumura, T., K. Koketsu, and K.-L.Wen, 2002, *Parallel PSM/FDM hybrid simulation of ground motions from the 1999 Chi-Chi*, *Taiwan*, *earthquake*, Pure and Applied Geophysics, in press

[5] Huang, 2000, *Two-dimensional reconstruction of the surface ground motions of an earthquake: the Semtember 21, 1999, Chi-Chi, Taiwan, Eathquake*, Geophys. Res. Lett., **27**, 3025-3028.

[6] Ishida, M., 1989, *The configuration of the Philippine Sea plate beneath the Kanto-Tokai district*, *Japan*, Abst. 25th IASPEI Meet.

[7] Kinoshita, S., *Kyoshin Net (K-NET)*, 1998, Seism. Res. Lett., **69**, 309--332.

[8] Kennett, B.L.N. and T. Furumura, 2002, *The influence of 3-D structure on the propagation of seismic waves away from earthquakes*, Pure and Applied Geophysics, in press.

[9] Koketsu, K. and Kukuchi, M., 2000, *Propagation of seismic ground motion in the Kanto basin, Japan*, Science, **288**, 1237--1239.

[10] Yagi, Y. and M. Kikuchi, 2000, *Source rupture process of the Tottori-ken Seibu earthquake of Oct. 6, 2000*, (*M*jma 7.3) *by using joint inversion of far-field and near-field waveform*, Abst. Seism. Soc. Japan 2000 Fall Meet., **T04**.

[11] Yamanaka, Y., M. Kikuchi and K. Yoshikawa, 2001, Source process of the 1946 Nankai earthquake (M8.0) and the 1964 Nigata earthquake (M7.5) inferred from JMA strong motion records, Abst. Seism. Soc. Japan 2001 Fall Meet., **C67**.

[12] Zhao, D.A., and A. Hasegawa, 1993, *P wave tomographic imaging of the crust an upper mantle beneath the Japan Islands*, J. Geophys. Res., **98**, 4333-4353.